PRODUCTION AND STUDY OF ANTIHYDROGEN IN THE ATHENA EXPERIMENT

P. Genova[a,b], M. Amoretti[c], C. Amsler[d], G. Bonomi[e], P. D. Bowe[f], C. Canali[c,g], C. Carraro[c,g], C. L. Cesar[h],M. Charlton[i], M. Doser[e], A. Fontana[a,b], M. C. Fujiwara[j,k], R. Funakoshi[k], J. S. Hangst[f], R. S. Hayano[k], L. V. Jørgensen[i], A. Kellerbauer[e], V. Lagomarsino[c,g], R. Landua[e], E. Lodi Rizzini[a,l], M. Macrí[c], N. Madsen[f], G. Manuzio[c,g], D. Mitchard[i], P. Montagna[a,b], H. Pruys,[e], C. Regenfus[e], A. Rotondi[a,b], G. Testera[c,g], A. Variola[c], L. Venturelli[a,l], Y. Yamazaki[j,m], D. P. van der Werf[i], N. Zurlo[a,l]

[a] *Dipartimento di Fisica Nucleare e Teorica, Università di Pavia, 27100 Pavia, Italy*

[b] *Istituto Nazionale di Fisica Nucleare, Sezione di Pavia, 27100 Pavia, Italy*

[c] *Istituto Nazionale di Fisica Nucleare, Sezione di Genova, 16146 Genova, Italy*

[d] *Physik-Institut, Zürich University, CH-8057 Zürich, Swtzerland*

[e] *PH Department, CERN, 1211 Geneva 23, Switzerland*

[f] *Department of Physics and Astronomy, University of Aarhus, 8000 Aarhus C, Denmark*

[g] *Dipartimento di Fisica, Università di Genova, 16146 Genova, Italy*

[h] *Instituto de Fisica, Universidade Federal do Rio de Janeiro, Rio de Janeiro 21945-970, Brazil*

[i] *Department of Physics, University of Wales Swansea, Swansea SA2 8PP, UK*

[j] *Atomic Physics Laboratory, RIKEN, Saitama 351-0198, Japan*

[k] *Department of Physics, University of Tokyo, Tokyo 113-0033, Japan*

[l] *Dipartimento di Chimica e Fisica per l'Ingegneria e per i Materiali, Università di Brescia, 25123 Brescia, Italy*

[m] *Graduate School of Arts and Sciences, University of Tokyo, Tokyo, 153-8902, Japan*

Abstract. In the last three years of data taking, the ATHENA experiment at the CERN Antiproton Decelerator facility has been able to produce large amounts of antihydrogen atoms and to study the formation process in detail. Moreover, in 2004, ATHENA tried to produce antihydrogen by means of laser stimulation. In this contribution we summarize the main results obtained and the progress made in analysing the results of the laser experiment.

T. Čechák et al. (eds.), Nuclear Science and Safety in Europe, 41–48.

1. Main goals of the experiment

The motivation for antihydrogen production is mainly related to two different kinds of study of great interest for fundamental physics: testing CPT symmetry in the H-$\overline{\mathrm{H}}$ system and studying the gravitational acceleration constant of $\overline{\mathrm{H}}$. The CPT theorem, which states the conservation of the product, in any order, of the three quantum operators T (time reversal), C (charge conjugation) and P (parity), is well established both theoretically and experimentally [1, 2, 3]. As a consequence of this theorem, for each particle there must be an antiparticle, that is a particle with opposite electric charge, opposite internal quantum numbers, opposite magnetic moment, same total lifetime and same inertial mass. The experimental tests of this theorem are based on high precision measurements of these quantities, in particular we recall the experiments on the mass difference between K and $\overline{\mathrm{K}^0}$ [3] and the charge-to-mass ratio difference between proton and antiproton [4].

With the mind open to new physics, one may look at the key assumptions of the CPT theorem and notice that it is based on the standard Quantum Field Theory - in particular it assumes point like space time - which may not be ultimately true. Moreover, there are theoretical models which, while preserving microcausality and renormalizability, violate CPT invariance, see e. g. [5]. The comparison of the spectral lines of antihydrogen with those of hydrogen provides a unique benchmark for a high precision CPT test. In the case of hydrogen, 10^{-14} precision has been achieved for 1s-2s spectroscopy [6]. A spectroscopic test is not model dependent as the K$\overline{\mathrm{K}^0}$ mass experiment, which assumes a standard model evolution of kaons to derive a suitable figure of merit to be compared with experimental data [7].

Another interesting topic is related to the gravitational behaviour of antiparticles inside the Earth's field. According to the Equivalence Principle the gravitational mass of a particle does not depend upon its properties, so it should be the same in the case of a particle or an antiparticle. Nevertheless no test of the gravitational mass of neutral antimatter has ever been done. Non standard theories have been proposed, implying differences in the gravitational mass of antiparticles with respect to particles, see [8, 9] for summaries of this work. A neutral system as antihydrogen, being free from disturbing effects due to the electric fields, is ideal to set reliable experimental limits to any antigravity evidence.

These two ultimate goals were not attained by the ATHENA experiment, although ATHENA was able to make the first step in this direction, by establishing the production of cold antihydrogen and making studies on the physical properties of the produced antiatoms.

2. Apparatus description and evidence for antihydrogen production

The apparatus used to produce and detect antihydrogen consists of three charged particle traps, of the Penning type, and an annihilation detector (for a detailed description of the ATHENA apparatus see [10]). On one side a trap is used to confine and cool the antiprotons coming from the Antiproton Decelerator (left side of figure 1), whereas on the other side the positrons coming from a 1.2 GBq radioactive ^{22}Na source are accumulated in a second Penning trap. In order to make antihydrogen both antiprotons and positrons are transferred and simultaneously confined in a third trap - the mixing trap - placed near the antiproton trap. The mixing and the antiproton trap electrodes are placed inside a 3 T superconducting magnet. The ambient temperature inside the mixing trap is around 15 K and the typical residual gas pressure is lower than 10^{-11} mbar. Usually in the mixing trap around 10^4 antiprotons interact with a positron plasma containing up to 10^8 positrons. The positron plasma is monitored by exciting its normal modes with a radiofrequency electric field. Typical parameters were 2.5 mm radius, 3.2 cm length and $2.5 \cdot 10^8$ cm^{-3} density [11, 12].

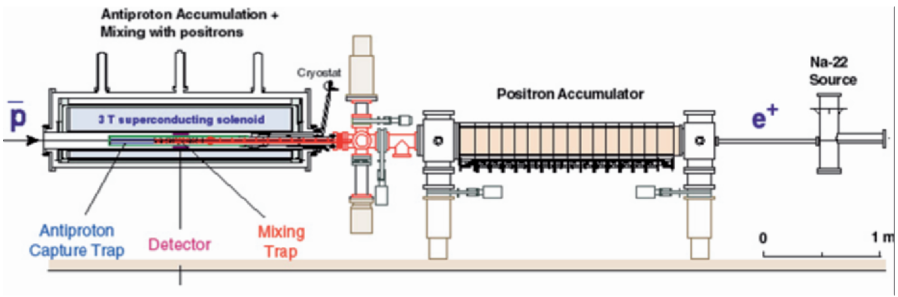

Figure 1. Sketch of the ATHENA apparatus.

The typical mixing procedure - *cold mixing* - consists of injecting first the positrons in the mixing trap and keeping them confined, then injecting the antiprotons and keeping the two clouds confined by using the so-called *nested trap* electrode potential configuration, see fig. 2 [13]. In this way the antiprotons can interact with the positron plasma. If $\overline{\mathrm{H}}$ is formed, it is not confined by the electric and magnetic fields and it moves along a straight line towards the trap electrodes, annihilating on them.

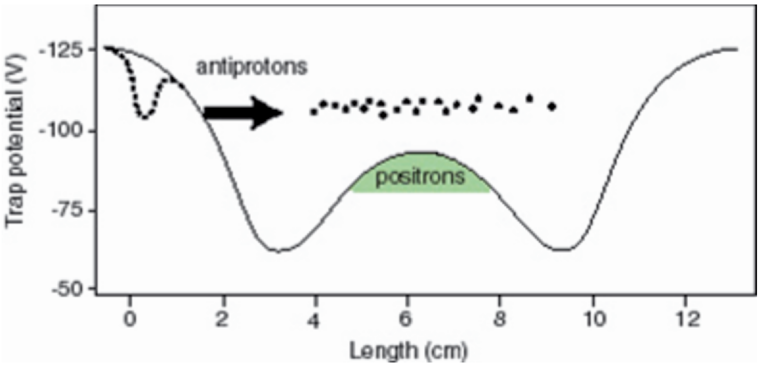

Figure 2. Nested trap potential configuration.

In order to detect antihydrogen production, the annihilation detector is placed just outside the trap electrodes. It consists of 2 layers of microstrip silicon detectors, for charged particle tracking, and 192 CsI crystals, which constitute a high granularity electromagnetic calorimeter (each crystal has dimensions 1.7 cm $\times$ 1.75 cm $\times$ 1.3 cm). The antihydrogen signature is the space and time coincidence of the nucleon-antiproton and electron-positron annihilations. The former annihilation produces neutral and charged pions, while the latter produces two back-to-back 511 keV photons. By using the silicon detectors, it is possible to reconstruct the charged pion tracks and hence the nucleon-antiproton annihilation vertex, while the 511 keV photons are detected by the calibrated crystals.

Given an antiproton annihilation vertex and two crystals hit by 511 keV photons, one may consider the distance between the centres of these two crystals and the antiproton vertex, expecting a small value in case of antihydrogen production. By considering the cosine of the angle between the segments joining the antiproton vertex with the 511 keV crystals' centres, one expects a peak at $\cos(\theta) = -1$ in case of antihydrogen production, but a uniform distribution otherwise. Figure 3 [14] shows the histogram of this variable for the standard *cold mixing* runs of 2002, superimposed with the so called *hot mixing* runs. In the *cold mixing* runs, we followed the standard procedure described here (positron temperature $\simeq$ 15 K), whereas in the *hot mixing* runs the positrons were heated with a radiofrequency electric field stimulating the quadrupole resonance mode (positron temperature up to $\simeq$ 3500 K). Due to the variation of the antihydrogen formation cross section - assuming it equal to the known hydrogen one - the higher the relative energy between the positrons and the antiprotons, the lower the antihydrogen formation probability. The *hot mixing* is thus a perfect

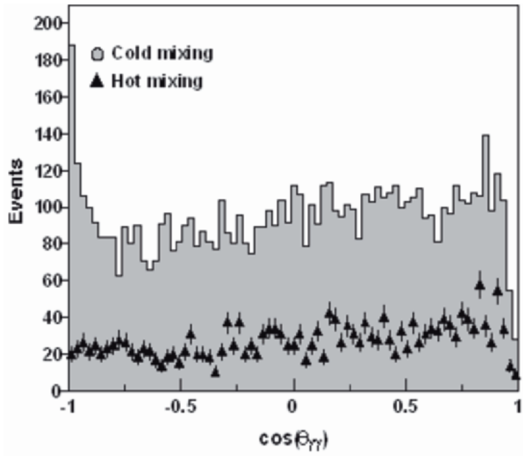

Figure 3. Opening angle distribution for *cold mixing* and *hot mixing* (triangles) [14].

background for antihydrogen production, having just the same conditions of *cold mixing*, with the $\overline{\mathrm{H}}$ signal totally suppressed. As fig. 3 shows, in experimental data, there is a clear $\overline{\mathrm{H}}$ signal for *cold mixing*, but no signal in case of *hot mixing*. Monte Carlo simulations of the detector are also in agreement with these data.

Further evidence of $\overline{\mathrm{H}}$ production is based on the different distributions of the annihilations in cases of *cold mixing* and *hot mixing*. In the former case a substantially isotropic distribution is observed with maximum intensity on a ring which corresponds to the trap wall, whereas for the latter the annihilations are mainly in the centre of the trap (see fig. 4). This is in agreement with antihydrogen production during *cold mixing* and no $\overline{\mathrm{H}}$ production during *hot mixing*, whose annihilations in the centre are $\overline{\mathrm{p}}$, not $\overline{\mathrm{H}}$, annihilations (possibly on residual gas or ions confined in the trap).

Furthermore the time distribution of the triggers is very different in the two cases (see fig. 5) with a peak followed by a gradual decay in case of *cold mixing*. The trigger distribution and the trigger peak rate have been studied at various heating intensities, i. e. heating the positron plasma with different RF voltages. This corresponds to different relative antiproton-positron energies, allowing a study of the dependence of antihydrogen production on the positron energy. The known $\overline{\mathrm{H}}$ formation mechanisms are the two-body - "spontaneous radiative" - recombination $\mathrm{e}^+ + \overline{\mathrm{p}} \rightarrow \overline{\mathrm{H}} + \gamma$ and the three-body recombination $\mathrm{e}^+ + \mathrm{e}^+ + \overline{\mathrm{p}} \rightarrow \overline{\mathrm{H}} + \mathrm{e}^+$. Since the cross sections of these processes scale differently with the positron temperature, the dominant process may be

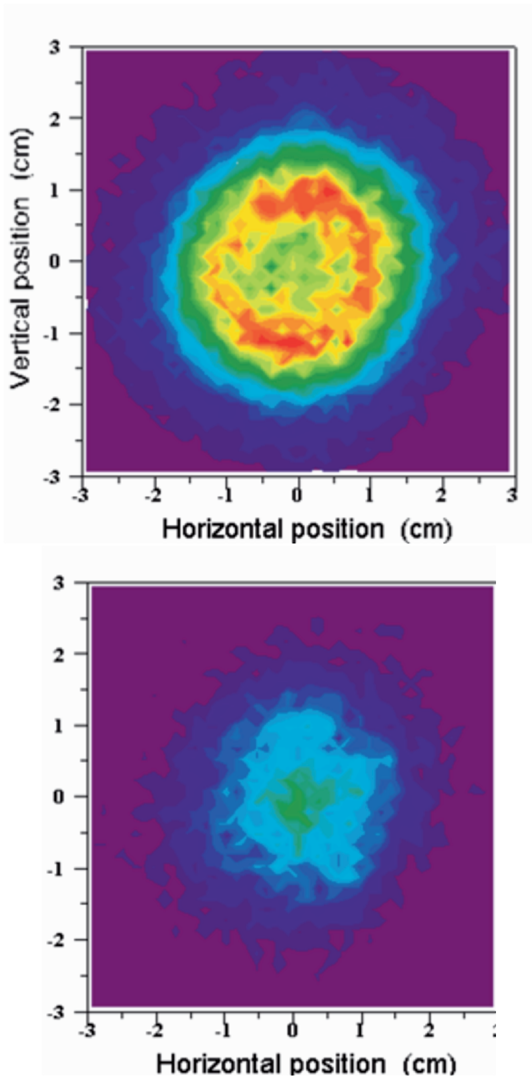

Figure 4. x-y vertex distribution for *cold mixing* - left - and *hot mixing* - right.

isolated by studying the temperature dependence. However, our data are not in agreement with a simple scaling law and the experimental peak rate is higher than the value expected by two-body process only [15]. This suggests a more complicated role of the recombination process, for which the scaling law is a rough approximation and whose theoretical calculation requires dedicated simulations to take properly into account, amongst other things, re-ionization processes and finite plasma dimensions [16].

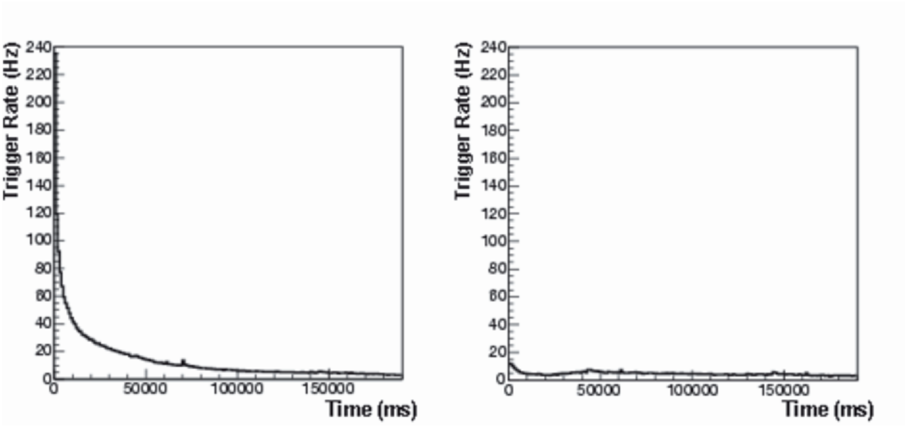

Figure 5. Trigger distribution for *cold mixing* - left - and *hot mixing* - right.

3. Laser stimulated recombination experiment

During 2004 we introduced a laser beam in the antihydrogen mixing region, in order to trigger the reaction $e^+ + \overline{p} + n\gamma \rightarrow \overline{H} + (n+1)\gamma$. We used a CO_2 continuous wave laser, tuned at 10.96 μm wavelength, to stimulate the transition from continuum to the $n = 11$ antihydrogen bound state. Theoretical studies on laser stimulated recombination indicate this frequency as well suited for enhanced production, with an expected stimulated rate higher than 60 Hz [17]. The laser is properly focused into the mixing region, with a peak intensity of 160 W/cm^2 at 10 W power, and chopped at a frequency of 25 Hz. In this way, during the same *cold mixing* run, it is possible to alternate laser ON and laser OFF conditions (presence/absence of the laser beam) and study the differences. During the laser runs, we observe a slight increase in the ambient temperature inside the nested trap and no vacuum deterioration.

In our preliminary analysis, we see no effect on the vertex temporal distribution due to the presence of the laser (the vertex distribution in the presence of the laser is statistically compatible with the distribution in the absence of the laser).

This result is confirmed by a study of the opening angle distribution for standard *cold mixing*, for laser ON and laser OFF data. There is still evidence of $\overline{H}$ production, but no clear enhancement. In the two samples the peaks at $\cos\theta = -1$ are compatible as well as the variable peak/*plateau*, the *plateau* being the average of the counts in the region $-0.9 < \cos\theta < 0.8$, where there is low $\overline{H}$ production (the analysis is still in progress).

4. Conclusion

We have breifly reviewed some interesting results obtained by the ATHENA experiment. $\overline{\mathrm{H}}$ production has been firmly established and the first studies on the produced antiatoms have been performed. No enhancement of $\overline{\mathrm{H}}$ production was obtained with a laser beam tuned at $\sim 11\ \mu m$, which seems to suggest that the dominant formation process is not the two-body one. These results and the ATHENA experience will be a useful guide and reference for the next generation of antihydrogen experiments.

References

1 G. Lüders, *Ann. Phys.* **21** (1957).
2 R. Jost, *Helv. Phys. Acta* **30** (1957).
3 A. Angelopoulos et al., *Phys. Lett.* **B471** (1999).
4 G. Gabrielse et al., *Phys. Rev. Lett.* **82** (1999).
5 R. Bluhm, V. A. Kostelecký, N. Russel, *Phys. Rev.* **D57** (1998).
6 M. Niering et al.,*Phys. Rev. Lett.* **84** (2000).
7 Shabalin E. 1994, *Phys. At. Nuclei* **57** (1994).
8 M. M. Nieto, *Phys. Rep.* **205** (1991).
9 M. M. Nieto, *Phys. Rep.* **216** (1992).
10 ATHENA Collab., M. Amoretti et al., *Nucl. Instr. Methods* **A518** (2004).
11 ATHENA Collab.: M. Amoretti et al., *Physics of Plasmas* **10** (2003).
12 ATHENA Collab.: M. Amoretti et al., *Phys. Rev. Lett.* **91** (2003).
13 G. Gabrielse, S. Rolston, L. Haarsma, W. Kells *Phys. Lett.* **A129** (1988).
14 ATHENA Collab.: M. Amoretti et al., *Nature* **419** (2002).
15 ATHENA Collab.: M. Amoretti et al., *Phys. Lett.* **B583** (2004) 59.
16 F. Robicheaux, *Phys. Rev.* **A70** (2004).
17 M. V. Ryabinina, L. Melnikov, *Nucl. Instr. Meth.* **B214** (2004).